Model Calculations of the Dynamic Susceptibility for the Modified Zener Model of Ferromagnetism and Comments on the Random-Phase Approximation*

L. C. Bartel
Sandia Laboratories, Albuquerque, New Mexico 87115
(Received 30 May 1973)

The transverse dynamic susceptibility for the modified Zener model of ferromagnetism is calculated in order to examine the behavior of neutron scattering resonances at low temperatures and at the Curie temperature T_C. The relationship of these calculations to those for a pure itinerant-electron ferromagnet is discussed. The inadequacy of the random-phase approximation in describing the behavior of the spin waves for Ni near T_C is also discussed.

Herring[1] suggested that the model proposed by Zener[2] for the ferromagnetism in mixed-valence transition-metal oxides may be applicable to describe the ferromagnetism in transition metals. The Zener model as applied to transition metals, referred to here as the modified Zener model (MZM), has been described at some length in papers by Arai and Parrinello[3] and Bartel.[4] The essential features of the model are a lattice of metal atoms, some with x d electrons and some with $(x+1)$ d electrons where the d shell is neither empty nor full; the x d electrons at each atomic site are coupled according to Hund's rule to yield the spin of maximum multiplicity; and the additional electron is itinerant and couples to the localized spin according to Hund's rule. The model is also appropriate for describing the ferromagnetism of an s-d exchange model where the d electrons produce the localized spin and the itinerant electrons are s-like.

The purpose of this paper is threefold. First, the behavior of the spin-wave (SW) resonances as they interact with the Stoner continuum and as the temperature nears the Curie temperature T_C will be examined. Secondly, the features peculiar to the MZM will be discussed. These goals will be accomplished through model calculations of the imaginary part of the transverse dynamic susceptibility which is related to the transverse inelastic neutron-scattering cross section.[5] The calculated behavior of the resonances energetically outside, near, and inside the Stoner continuum will be discussed. As far as I am aware, the report of calculations of the resonance line shapes for $T = T_C$ is the first of its kind for either a MZM or a pure itinerant-electron ferromagnet. Finally, the inadequacies of the random-phase approximation (RPA) as applied to Ni will be pointed out.

In the MZM the itinerant electrons are treated using a Hubbard-model Hamiltonian H_H, and the itinerant electron couples to the localized spin $\vec{S}$ by a term $-2J\vec{\sigma}_i \cdot \vec{S}_i$, where $\vec{\sigma}_i$ is the itinerant-electron-spin operator for an electron on site i and J is the interaction parameter. The Hamiltonian for the MZM is H_H plus a term which is a sum over the lattice sites of the above interaction term.[4] The transverse inelastic neutron scattering cross section is related to the imaginary part of the transverse dynamic susceptibility $\chi^{+-}(\vec{q}, \omega)$ which in turn is related to the transverse-spin Green's function for the itinerant electrons.[4,5] Here $\vec{q}$ is the wave vector and ω is the angular frequency. In Ref. 4 the methods and decoupling procedures used by Doniach and Wohlfarth[6] and Izuyama *et al.*[5] were employed with the result that in the RPA the Green's function is given by Eq. (18) of Ref. 4 and $\chi^{+-}(\vec{q}, \omega)$ becomes[4]

$$\chi^{+-}(\vec{q}, \omega) = \frac{-(2\pi)^{-1}\chi^0(\vec{q}, \omega)}{1-[I-2J^2\bar{S}/(\hbar\omega - Jn\zeta)]\chi^0(\vec{q}, \omega)}, \quad (1)$$

where I is the Coulomb repulsion energy parameter for electrons of opposite spin localized on the same site in H_H, $n\zeta$ is the itinerant-electron polarization, and $\bar{S}$ is the localized-spin polarization which is assumed to be the same at all sites. The unenhanced susceptibility $\chi^0(\vec{q}, \omega)$ is given by

$$\chi^0(\vec{q}, \omega) = -N^{-1}\sum_{\vec{k}} \frac{n_{\vec{k}+\vec{q}\uparrow} - n_{\vec{k}\downarrow}}{\hbar\omega - (\epsilon_{\vec{k}} - \epsilon_{\vec{k}+\vec{q}}) - \Delta}, \quad (2)$$

where

$$\Delta = In\zeta + 2J\bar{S} \quad (3)$$

is the Stoner splitting, where $n_{\vec{k}\sigma}$ is the thermal average of the electron number operator, and here $\epsilon_{\vec{k}}$ is the single-band fcc tight-binding energy described by Eq. (45) of Ref. 4. The susceptibility given by Eq. (1) is an exchange enhanced susceptibility where the effective exchange constant now depends on ω

$$I_{eff}(\omega) = I - 2J^2\bar{S}/(\hbar\omega - Jn\zeta).$$

There are two types of resonances determined by the singularities in $\chi^{+-}(\vec{q}, \omega)$. SW excitations occur when the values of $\vec{q}$ and ω do not produce a branch cut in $\chi^0(\vec{q}, \omega)$, and single-particle or Stoner excitations occur when the values of $\vec{q}$ and

ω produce a branch cut in $\chi^0(\vec{q}, \omega)$.[5] Since there are two inequivalent spin systems in the MZM, localized, and itinerant electron, one expects, and it has been demonstrated in Ref. 4, that there should be an acoustic and an optic branch to the SW spectrum. The energies for the acoustic and optic branches are[4]

$$\hbar\omega_{ac}(\vec{q}) = Dq^2, \quad \text{acoustic branch,}$$
$$\hbar\omega_{op}(\vec{q}) = \hbar\omega_0 + D(I\hbar\omega_0/J\Delta - 1)q^2, \quad \text{optic branch,} \tag{4}$$

where

$$\hbar\omega_0 = E_{op} = Jn\zeta + 2J\bar{S} \tag{5}$$

and D can be determined from Refs. 5 and 6. The dispersion curve, including the two SW branches and the Stoner excitations, is shown schematically in Fig. 1. The existence of an acoustic branch *does not* depend upon the coupling of an itinerant electron and a localized spin and exists even if $J = 0$ or $\vec{S} = 0$. An acoustic branch has been observed in some transition metals and alloys.[7-11] The SW dispersion curve for a pure itinerant-electron ferromagnet ($J = 0$ or $\vec{S} = 0$) would be similar to that of the MZM, Fig. 1, except that there would not be an optic branch and the acoustic branch would have larger initial values (larger D) and a higher maximum energy than for the MZM. On the other hand, the optic branch *does* depend on the coupling of an itinerant electron to a localized spin. As far as I am aware, the optic branch has not been observed in itinerant electron ferromagnets of the type discussed here. The reasons for the failure to observe the optic branch may be that (i) the energy E_{op} is too large and outside the range of normal neutron energies (it is estimated that $E_{op} \gtrsim 0.1$ eV) or (ii) the optic branch energy is too close to that of the Stoner excitations and thus these are not well defined excitations as will be shown. The dashed portions of the curves in Fig. 1 signify that the SW excitations are not well defined excitations as they "enter" the Stoner continuum.

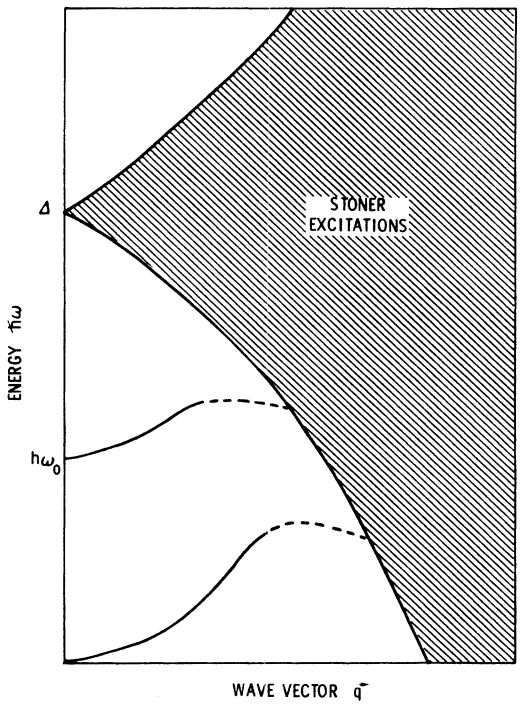

FIG. 1. Schematic drawing of the excitation spectrum for the modified Zener model. Shown are the acoustic and optic spin-wave branches and the continuum of Stoner excitations. The dashed portions of the curves indicate that the excitations are not well defined. Here Δ is the Stoner splitting, Eq. (3), $\hbar\omega_0$ is the $\vec{q} = 0$ optic branch energy, Eq. (5), and it is assumed in the figure that $I > J$.

The imaginary part of the dynamic susceptibility is found by solving for the imaginary part of $\chi^{+-}(\vec{q}, \omega + i0)$. For $\omega \to \omega + i0$, $\chi^0(\vec{q}, \omega + i0)$ becomes complex

$$\chi^0(\vec{q}, \omega + i0) = [\chi^0(\vec{q}, \omega)] + i[\chi^0(\vec{q}, \omega)]'',$$

where $[\chi^0(\vec{q}, \omega)]'$ is the principal part of the sum in Eq. (2) and $[\chi^0(\vec{q}, \omega)]''$ is given by

$$[\chi^0(\vec{q}, \omega)]'' = \pi N^{-1} \sum_{\vec{k}} [n_{\vec{k}+\vec{q}\uparrow} - n_{\vec{k}\downarrow}] \delta(\hbar\omega - (\epsilon_{\vec{k}} - \epsilon_{\vec{k}+\vec{q}}) - \Delta). \tag{6}$$

$[\chi^0(\vec{q}, \omega)]''$ is the density of Stoner states. When $\vec{q}$ and ω are such that $[\chi^0(\vec{q}, \omega)]'' = 0$, the resonances are outside the Stoner continuum and are of the SW variety. These SW resonances are extremely sharp; therefore, to give these resonances a finite width and intensity, a small phenomenological damping parameter Γ will be assumed. From Eq. (1) the $\mathrm{Im}\chi^{+-}(\vec{q}, \omega + i0)$ becomes

$$\mathrm{Im}\chi^{+-}(\vec{q}, \omega + i0) = \frac{[\chi^0(\vec{q}, \omega)]''}{\{1 - I_{\mathrm{eff}}(\omega)[\chi^0(\vec{q}, \omega)]'\}^2 + \{I_{\mathrm{eff}}(\omega)[\chi^0(\vec{q}, \omega)]''\}^2}. \tag{7}$$

For $\vec{q}$ and ω such that there is no branch cut in $\chi^0(\vec{q}, \omega)$, $[\chi^0(\vec{q}, \omega)]''$ is replaced by a constant Γ.

In order to be able to calculate $[\chi^0(\vec{q}, \omega)]'$ and $[\chi^0(\vec{q}, \omega)]''$, it is necessary to determine self-consistency $n\zeta$, $\bar{S}$, and the Fermi energy E_F. This was accomplished using Eqs. (15), (16), (24)–(26), and (45) of Ref. 4 and techniques outlined in Ref. 4. The summation for $[\chi^0(0, 0)]'$ is in agreement (to within ~2%) with the exact value of $n\zeta/\Delta$. Extrapolated and smoothed values of $[\chi^0(\vec{q}, \omega)]'$ were used in the calculation of $\mathrm{Im}\chi^{+-}(\vec{q}, \omega + i0)$, since the position and shape of the resonances are extremely sensitive to the values of $[\chi^0(\vec{q}, \omega)]'$ used.

In the model calculation to be discussed below, the behavior of the SW resonances will be examined for the case when there is no Stoner gap at the zone

boundary (i.e., the Stoner continuum intersects the $\hbar\omega = 0$ axis for a $|\vec{q}| < |\vec{q}_{max}|$). The dispersion curve is illustrated in Fig. 1. To illustrate the behavior of $\mathrm{Im}\chi^{+-}(\vec{q}, \omega)$, J was taken less than I, and from a close examination of Eqs. (1) and (4) it is clear that $0 \leq \hbar\omega_{ac} < Jn\zeta$ and $Jn\zeta < \hbar\omega_{op} < \Delta$. In the regime of $\vec{q}$ and ω such that $[\chi^0(\vec{q}, \omega)]'' = 0$, a damping parameter Γ was chosen somewhat arbitrarily. It was found that the resonances became sharper and more intense and the sloping background became less pronounced for the smaller values of Γ that were used.

The behavior of the acoustic-branch and optic-branch resonances for the MZM, determined from Eq. (7), as functions of ω for various $\vec{q}$ in the [100] direction are illustrated in Figs. 2 and 3, respectively. Upon examination of Eq. (1), a significant decrease in $\mathrm{Im}\chi^{+-}(\vec{q}, \omega)$ as $\hbar\omega/J \sim n\zeta$ ($n\zeta \sim 0.4$) would be a characteristic of the MZM and would not be the case for a pure itinerant-electron ferromagnet ($J = 0$ or $S = 0$). However, the resonance is well

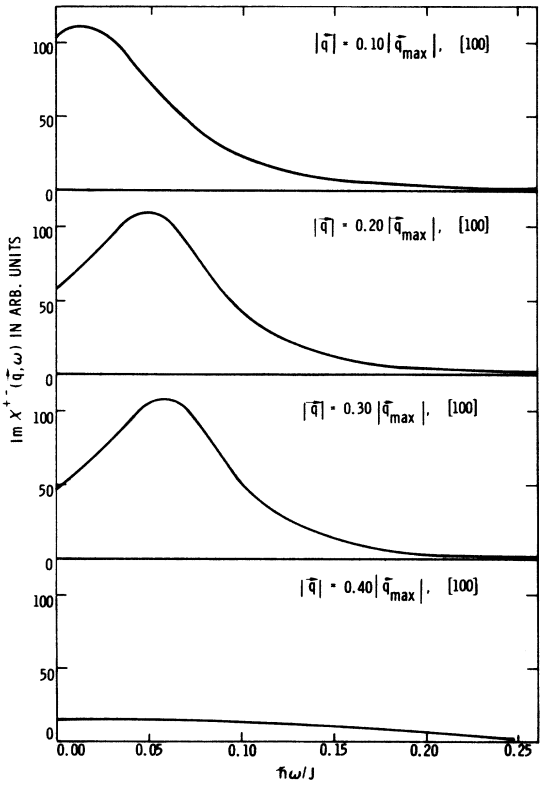

FIG. 2. $\mathrm{Im}\chi^{+-}(\vec{q}, \omega)$ as a function of $\hbar\omega/J$ at $T = 0$ for various $\vec{q}$. The resonances are the acoustic branch spin-wave resonances. For the top three curves the resonances are outside the Stoner continuum while for the bottom curve any resonance would be inside the Stoner continuum. Γ was chosen to be equal to J for this figure and $I/J = 90$.

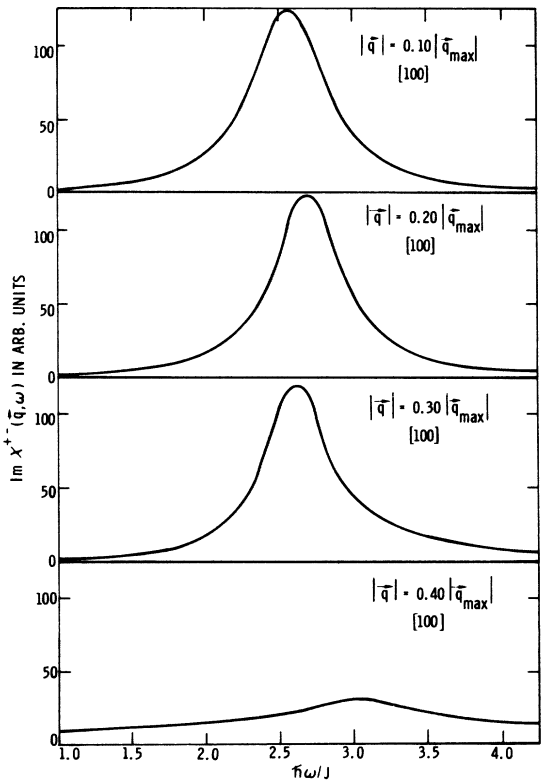

FIG. 3. $\mathrm{Im}\chi^{+-}(\vec{q}, \omega)$ as a function of $\hbar\omega/J$ at $T = 0$ for various $\vec{q}$. The resonances are the optic-branch spin-wave resonances. For the top three curves the resonances are outside the Stoner continuum while for the bottom curve the weak resonance is inside the Stoner continuum. Γ was chosen to be equal to J for this figure and $I/J = 90$.

away from this point, $\hbar\omega/J = n\zeta$, such that the anticipated decrease would probably not be observable. (The pure itinerant-electron ferromagnet will be referred to as the $J = 0$ case.) The sloping background to the resonance is a characteristic of the MZM as well as when $J = 0$, and the amount of slope depends upon the choice of Γ. A characteristic of the acoustic and optic branches for the MZM and the acoustic branch for $J = 0$ is that as the SW excitation approaches the Stoner continuum the resonance is repelled somewhat. This behavior is illustrated by comparing the $|\vec{q}| = 0.30|\vec{q}_{max}|$ curve with the $|\vec{q}| = 0.10|\vec{q}_{max}|$ and $0.20|\vec{q}_{max}|$ curves of Figs. 2 and 3. For $|\vec{q}| = 0.40|\vec{q}_{max}|$ the SW has entered the Stoner continuum and for the acoustic branch, Fig. 2, $\mathrm{Im}\chi^{+-}(\vec{q}, \omega)$ does not show a resonance; whereas, for the optic branch, Fig. 3, a very broad and very weak resonance is apparent. Inside the Stoner continuum $[\chi^0(\vec{q}, \omega)]'' \neq 0$ and depends upon $\vec{q}$ and ω and is not in general a constant. The widths, intensities, and the sloping background for the resonances out-

side the Stoner continuum depend upon the choice of Γ.

In Fig. 4 the behavior of $\mathrm{Im}\chi^{+-}(\vec{q}, \omega)$ for the MZM as a function of $\vec{q}$ in the [100] direction for various $\hbar\omega/J$ ($\hbar\omega/J < n\zeta$) is illustrated. For $\hbar\omega/J < 0.06$ the resonances are well outside the Stoner continuum. The behavior of the resonance just outside the Stoner continuum is illustrated by the $\hbar\omega/J = 0.06$ curve. When $\hbar\omega/J = 0.10$ the resonant condition, $I_{\mathrm{eff}}(\omega)[\chi^0(\vec{q}, \omega)]' = 1$, is not satisfied; however, $\mathrm{Im}\chi^{+-}(\vec{q}, \omega)$ still shows some sort of maximum. The characteristic feature of $\mathrm{Im}\chi^{+-}(\vec{q},\omega)$ becoming very small at a $\vec{q}(|\vec{q}|/|\vec{q}_{\max}| \sim 0.36)$ corresponding to the entering of the SW excitations into the Stoner continuum is common to the MZM and the $J = 0$ case. This decrease is due in part to a maximum in $[\chi^0(\vec{q}, \omega)]'$ as a function of $\vec{q}$ for a fixed ω at the entry point into the Stoner continuum. The behavior of $\mathrm{Im}\chi^{+-}(\vec{q}, \omega)$ inside the Stoner continuum is illustrated in Fig. 4 when $|\vec{q}|/|\vec{q}_{\max}| \gtrsim 0.36$.

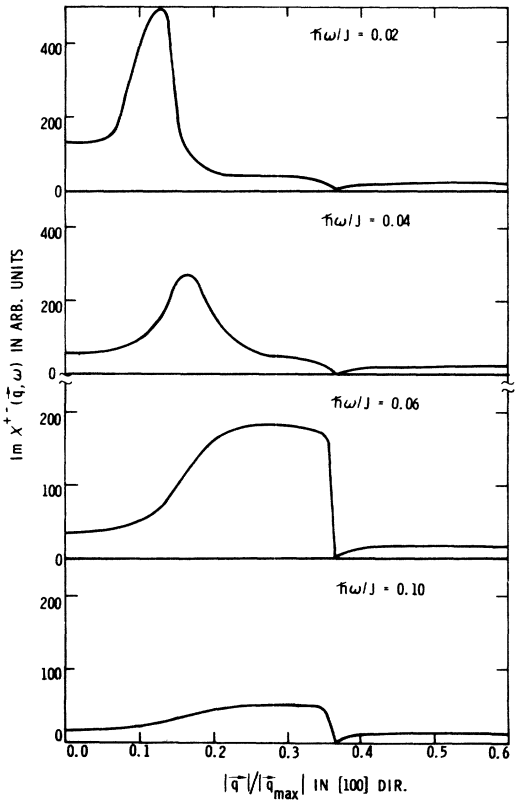

FIG. 4. $\mathrm{Im}\chi^{+-}(\vec{q}, \omega)$ as a function of $|\vec{q}|/|\vec{q}_{\max}|$ at $T = 0$ for various ω. Behavior of the acoustic-branch spin-wave resonances as they enter the Stoner continuum is illustrated. $\mathrm{Im}\chi^{+-}(\vec{q}, \omega)$ is in the Stoner continuum for $|\vec{q}| \gtrsim 0.36\,|\vec{q}_{\max}|$. For $\hbar\omega/J = 0.10$ the resonant condition in Eq. (7) is not satisfied. Γ was taken equal to $\hbar\omega/J$ and $I/J = 90$ in each curve. Note the change in scale in the figure.

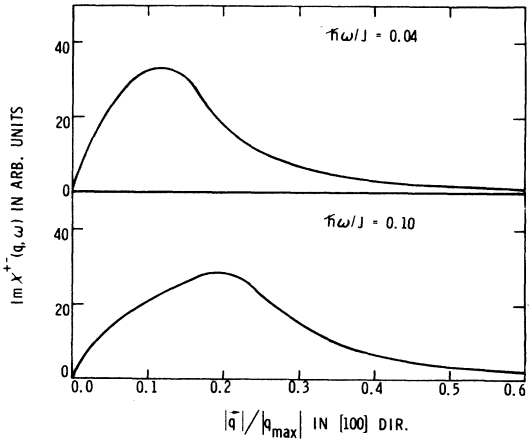

FIG. 5. $\mathrm{Im}\chi^{+-}(\vec{q}, \omega)$ as a function of $|\vec{q}|/|\vec{q}_{\max}|$ at $T = T_C$ for two ω's. Representation of the behavior of the resonances at $T = T_C$, where $\mathrm{Im}\chi^{+-}(\vec{q}, \omega)$ is inside the Stoner continuum for the $\vec{q}$'s and ω's shown. Here $I/J = 90$.

The behavior of the acoustic branch resonances for the MZM and for the $J = 0$ case is very similar. (For $J = 0$ there is no optic branch.) The calculated behavior of the resonances, the sloping background, and the reduction in intensity as the SW enters the Stoner continuum are in agreement with experimental results.[8,9]

Finally, the characteristic features of $\mathrm{Im}\chi^{+-}(\vec{q},\omega)$ for the MZM at $T = T_C$ are illustrated in Fig. 5. The $J = 0$ case would have similar features. The resonances are extremely broad and very weak in intensity. The SW constant D, Eq. (4), is temperature dependent leading to a change in the dispersion curve and for a fixed energy would lead to a change in the position of the resonance in $\vec{q}$ space. The resonances in Fig. 5 show this change. The behavior of $\mathrm{Im}\chi^{+-}(\vec{q}, \omega)$ at $T = T_C$ is drastically affected by the vanishing of the Stoner splitting Δ at $T = T_C$. The dependence of the Stoner splitting on the magnetization $n\zeta$ and/or $\bar{S}$ is a direct consequence of the RPA used to obtain a solution for $\chi^{+-}(\vec{q}, \omega)$.

Even though the applicability of the MZM to Fe and Ni has not been established, it is instructive to compare experimental results on the materials to the predictions of this paper for the acoustic branch SW's. Measurements of the SW spectra of Fe and Ni[7-9] at $T < T_C$ show the disappearance of the resonances as the SW's enter the Stoner continuum in a manner similar to that illustrated by the model calculations. Measurements for Fe[10] as $T \to T_C$ show that D is temperature dependent and that resonances as a function of energy $|\vec{q}| = 0.1$ Å^{-1} collapse to zero energy as $T \to T_C$. It ap-

pears that for Fe the behavior of the inelastic neutron scattering for $T \to T_C$ differs from that at lower temperatures in agreement with predictions based on the model calculations of this paper.

The recent measurements for Ni[9] show that at the *larger* $\vec{q}$ values D, the resonance width and intensity, and the energy boundary of the Stoner continuum appear to remain more or less unaffected as $T \to T_C$. At $T < T_C$ the observance of the disappearance of the resonances as the SW's enter the Stoner continuum establishes the existence of the band of single particle excitations as predicted. However, for $T \to T_C$ and for $T > T_C$ the measurements[9] indicate that the SW resonances for Ni do not vanish which is contrary to the predictions of the model calculations of this paper.

Recently, Cooke and Davis[12] have made a more realistic calculation of $\mathrm{Im}\chi^{+-}(\vec{q}, \omega)$ for Ni using essentially a pure itinerant-electron model. In their calculations they used a wave-vector-dependent exchange energy $I(\vec{q})$ and used a realistic band structure for Ni. They obtain good agreement between the calculated and experimental[9] SW energies at low T. However, they used a form of an RPA calculation and their results are that the Stoner splitting, which is a function of $\vec{q}$, vanishes at $T = T_C$ just as in this paper. Therefore, it appears that even these more elaborate calculations cannot explain the behavior of $\mathrm{Im}\chi^{+-}(\vec{q}, \omega)$ for $T \to T_C$ in Ni. The culprit of course is the simple RPA. Mean-field theories, of which the RPA and Hartree-Fock approximation are a part, produce excitation energies for which the scaling with temperature is $\vec{q}$ independent and predict that short-wavelength and long-wavelength SW's renormalize in the same way.

Recently, Lines[13] has investigated an improved Green's function decoupling procedure for the Heisenberg model which renormalizes the long-wavelength SW's according to the magnetization and the short-wavelength SW's according to the nearest-neighbor spin-correlation function. A critical wave vector is defined as $q_c = \pi/L$, where L is some sort of coherence length for which SW's with $q > q_c$ experience much less damping and renormalization than do SW's with $q < q_c$.[13] At $T = T_C$ the long-wavelength SW's would vanish; whereas, the short-wavelength SW's do not necessarily vanish. It seems that a decoupling procedure in the spirit of that used by Lines[13] would be appropriate for itinerant-electron ferromagnets. Clearly, the simple RPA, which fails to take into account some very important electron correlations, is not appropriate to describe the ferromagnetism in at least Ni and more work is needed to include these correlations for the larger $\vec{q}$ values.

---

*Work supported by the U. S. Atomic Energy Commission.

[1]C. Herring, in *Magnetism*, edited by G. T. Rado and H. Suhl (Academic, New York, 1966), Vol. IV, pp. 123–125, 182–186.
[2]C. Zener, Phys. Rev. **82**, 403 (1951).
[3]T. Arai and M. Parrinello, Phys. Rev. Lett. **27**, 1226 (1971).
[4]L. C. Bartel, Phys. Rev. B **7**, 3153 (1973).
[5]T. Izuyama, D. Kim, and R. Kubo, J. Phys. Soc. Jap. **18**, 1025 (1963).
[6]S. Doniach and E. P. Wohlfarth, Proc. R. Soc. A 296, 442 (1967).
[7]H. A. Mook, R. M. Nicklow, E. D. Thompson, and M. K. Wilkinson, J. Appl. Phys. **40**, 1450 (1969).
[8]H. A. Mook and R. M. Nicklow, Phys. Rev. B **7**, 336 (1973).
[9]H. A. Mook, J. W. Lynn, and R. M. Nicklow, Phys. Rev. Lett. **30**, 556 (1973).
[10]G. Shirane, V. J. Minkiewicz, and R. Nathans, J. Appl. Phys. **39**, 383 (1968).
[11]F. Menzinger, G. Caglioti, G. Shirane, R. Nathans, S. J. Pickart, and H. A. Alperin, J. Appl. Phys. **39**, 455 (1968).
[12]J. F. Cooke and H. L. Davis, AIP Conf. Proc. **10**, 1218 (1972).
[13]M. E. Lines, Phys. Rev. B **3**, 1749 (1971).